
# AFRL-RH-BR-TR-2009-0053

# Drug-mediated Laser Photo Damage of Globular Proteins

**Lorenzo Brancaleon**
**Department of Physics and Astronomy**
**University of Texas at San Antonio**
**One UTSA Circle, San Antonio, TX 78249**

**March 2009**

**Final Report for 10 July 2007 - 10 Mar 2009**



**Distribution A; Approved for public release; distribution unlimited; Public Affairs Case file number 09-467, 29 September 2009; Brooks City-Base, Texas 78235.**

**Air Force Research Laboratory**
**711 Human Performance Wing**
**Human Effectiveness Directorate**
**Directed Energy Bioeffects Division**
**Optical Radiation Branch**
**Brooks City-Base, TX 78235**

# NOTICE AND SIGNATURE PAGE

Using Government drawings, specifications, or other data included in this document for any purpose other than Government procurement does not in any way obligate the U.S. Government. The fact that the Government formulated or supplied the drawings, specifications, or other data does not license the holder or any other person or corporation; or convey any rights or permission to manufacture, use, or sell any patented invention that may relate to them.

This report was cleared for public release by the 311th Public Affairs Office at Brooks City Base, TX, and is available to the general public, including foreign nationals. Copies may be obtained from the Defense Technical Information Center (DTIC) (http://www.dtic.mil).

AFRL-RH-BR-TR-2009-0053 HAS BEEN REVIEWED AND IS APPROVED FOR PUBLICATION IN ACCORDANCE WITH ASSIGNED DISTRIBUTION STATEMENT

_____//SIGNED//_____
Robert J. Thomas, PhD USAF
Work Unit Manager
711 HPW/ RHDO

_____//SIGNED//_____
GARRETT D. POLHAMUS, Ph.D.
Chief, Directed Energy Bioeffects Division
Human Effectiveness Directorate
711 Human Performance Wing
Air Force Research Laboratory

This report is published in the interest of scientific and technical information exchange, and its publication does not constitute the Government's approval or disapproval of its ideas or findings.

# REPORT DOCUMENTATION PAGE

*Form Approved*
*OMB No. 0704-0188*



| 1. REPORT DATE *(DD-MM-YYYY)* | 2. REPORT TYPE | 3. DATES COVERED *(From - To)* |
|---|---|---|
| March 2009 | Final Technical Report | 10 July 2007 - 10 Mar 2009 |

**4. TITLE AND SUBTITLE**

**Drug-mediated Laser Photo Damage of Globular Proteins**

**5a. CONTRACT NUMBER**

**5b. GRANT NUMBER**
FA8650-07-1-6850

**5c. PROGRAM ELEMENT NUMBER**
62202F

**6. AUTHOR(S)**

Lorenzo Brancaleon

**5d. PROJECT NUMBER**
7757

**5e. TASK NUMBER**
B2

**5f. WORK UNIT NUMBER**
35

**7. PERFORMING ORGANIZATION NAME(S) AND ADDRESS(ES)**

Air Force Research Laboratory
711 Human Performance Wing
Human Effectiveness Directorate
Directed Energy Bioeffects
Optical Radiation Branch
Brooks City-Base, TX 78235-5214

Department of Physics and Astronomy
University of Texas at San Antonio
One UTS Circle, San Antonio TX, 78249

**8. PERFORMING ORGANIZATION REPORT**

UTSA
711 HPW/ RHDO

**9. SPONSORING / MONITORING AGENCY NAME(S) AND ADDRESS(ES)**

Air Force Research Laboratory
711 Human Performance Wing
Human Effectiveness Directorate
Directed Energy Bioeffects
Optical Radiation Branch
Brooks City-Base, TX 78235-5214

**10. SPONSOR/MONITOR'S ACRONYM(S)**

711 HPW/RHDO
UTSA

**11. SPONSOR/MONITOR'S REPORT NUMBER(S)**

AFRL-RH-BR-TR-2009-0053

**12. DISTRIBUTION / AVAILABILITY STATEMENT**

Distribution A; Approved for public release; distribution unlimited; Public Affairs case file number 09-467, 29 Sep 09.

**13. SUPPLEMENTARY NOTES**

**14. ABSTRACT**

The research activity carried out as part of this funded project studied the mechanisms of interaction of two porphyrins (protoporphyrin IX (PPIX)) and tetra-sulfonatophenyl-porphyrin (TPPS)) with two globular proteins (β-lactoglobulin (BLG) and tubulin) and the effect that the irradiation of the porphyrins produce on the conformation of the two proteins. We established that both porphyrin can bind the proteins. However while PPIX binding to BLG is modulated by the pH of the solution, the binding of TPPS is not. In combination with computational data we have established that both porphyrins bind to superficial but separate sites which are controlled by different interactions (van der Waals for PPIX, purely Coulombian for TPPS). We found that binding by itself does not produce conformational changes in the proteins but that, in the case of BLG, TPPS increases the stability of the protein to denaturation.

Finally we have established that irradiation of both porphyrin produces conformational changes in BLG. The changes are smaller (< 10%) for the BLG/PPIX complex and larger (> 15%) for the BLG/TPPS complex. They can be summarized as partial unfolding of the β-structure of the protein into an unstructured arrangement. The unfolding is not dependent on the presence of molecular oxygen and does not appear to be caused by a temperature change induced by the relaxation of the porphyrin. This leads us to conclude that the unfolding is likely caused by photo-induced electron transfer between the porphyrin and the protein that triggers subsequent unfolding of the polypeptide. This, in the case of TPPS, is accompanied by a chemical modification of one of the Trp residues of the protein, which confirms the charge-transfer mechanism.

Overall, our results are very promising and further studies would be dedicated to investigate whether porphyrins can be used as agents for chromophore-assisted laser inactivation of proteins (CALI). This method could then be used to employ laser light in order to selectively inactivate proteins and receptors in living cells. This could be applied to many biomedical and biochemical studies of cellular pathways and it could also be applied in the future to clinical settings.

**15. SUBJECT TERMS**

| 16. SECURITY CLASSIFICATION OF: | | | 17. LIMITATION OF ABSTRACT | 18. NUMBER OF PAGES | 19a. NAME OF RESPONSIBLE PERSON |
|---|---|---|---|---|---|
| | | | | | Robert Thomas |
| a. REPORT | b. ABSTRACT | c. THIS PAGE | SAR | 38 | 19b. TELEPHONE NUMBER *(include area code)* |
| U | U | U | | | |

**Standard Form 298 (Rev. 8-98)**
**Prescribed by ANSI Std. 239.18**

This Page Intentionally Left Blank

# Table of Contents



# Table of Figures

# List of Tables

# 1 INTRODUCTION

The objective of this research was to investigate whether the visible-light irradiation of light-activated drugs, non-covalently bound to globular proteins, would prompt changes of the polypeptide due to photophysical/photochemical events initiated by the ligand.

There is mounting evidence that molecular mechanisms initiated by light-activated drugs in cells are more sophisticated than initially thought ,[1] and involve both relocalization of the dyes during light exposure and the direct targeting of proteins.[1,2] Among the targeted proteins arguably the most significant is tubulin and, consequently, the microtubules (MT). *In vivo*, photodamage mediated by the irradiation of porphyrins, produces destabilization of MT with consequent arrest of the cell cycle and apoptosis.[2] [3] The mechanism of a light-activated drug's photodamage of proteins is poorly understood.

Besides biomedical applications, laser-induced conformational changes of proteins could have an impact in other basic as well as technological areas of research. Controlling protein photodamage could in fact lead to (i) the fabrication of covalent and/or non-covalent molecular switches,[4] (ii) the fabrication of light-based biosensor that link light absorption with mechanical effects in the proteins and (iii) sophisticated methods to unfold proteins in more physiological conditions for the investigation of folding/unfolding protein dynamics.[5] The study would be particularly relevant if the induced photodamage was produced on generic globular protein, which does not contain specific active sites for the light-activated drugs.

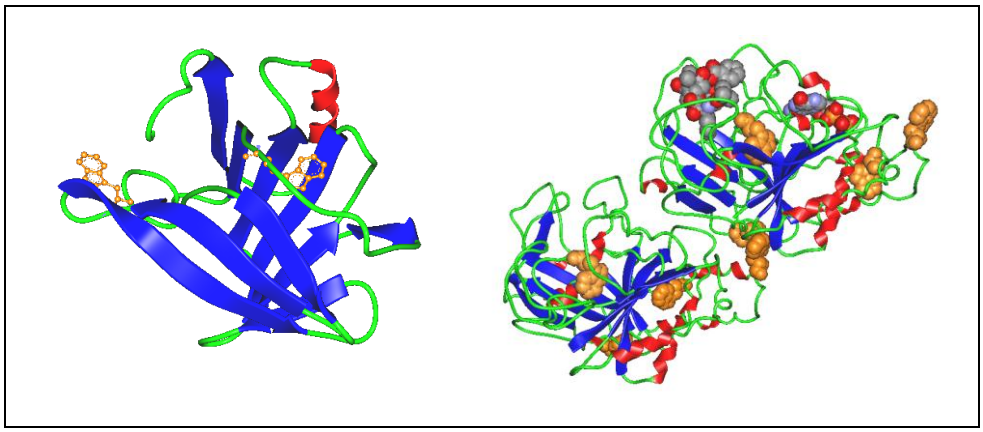

**Figure 1 Structure of BLG (left) and $\alpha\beta$ tubulin heterodimer (right)**

For this reason, we used two model globular proteins: $\beta$-lactoglobulin (BLG) and tubulin. BLG is a small globular protein of 162 amino acids with a $\beta$-barrel motif (Figure 1). Its physiological role has not been entirely clarified. However, it is known that BLG binds many different hydrophobic ligands, including hydrophobic porphyrins. Tubulin is a ~ 55 KDa protein which is normally found as a heterodimer of $\alpha$ and $\beta$ forms[6] (Figure 1). *In vivo*, tubulin heterodimers assemble reversibly to create MT[7] which are essential for diverse functions including intracellular signaling, morphology and cell division.[7] The *in vivo* assembly depends on the presence of nucleotides and Microtubule Associated Proteins (MAP),[7] but it has been shown that

tubulin aggregation and stabilization can be prompted by several exogenous molecules such as taxoids and statins.[8]

The fact that some porphyrins such as TSPP and other porphyrins produce similar stabilization is intriguing. Moreover, the molecular effects of porphyrins on tubulin and MT is still debated since both stabilization and destabilization of MT has been claimed.[2,9] This makes the problem even more interesting because different porphyrins may bind at different sites and produce different results on the protein. Despite this initial evidence, the molecular mechanisms of porphyrin-induced effects on tubulin have not been thoroughly characterized.

Modifications of protein structure through reaction with transient excited states (such as those that may be produced by irradiating porphyrin molecules) has been thoroughly documented using pulse radiolysis,[10] although many of the specific mechanisms involving the secondary and tertiary structures remain unknown. Even less information is available on the effects that non-ionizing radiation can produce especially when the transient excited states are formed by polyacrylamide (PAM) directly attached to the proteins. We believe that a good model to investigate this problem is to study the effects of porphyrin irradiation on globular proteins which do not offer active sites for the porphyrin ligands. The photophysical and photochemical properties of porphyrins are likely to produce structural effects on tubulin upon absorption of light. It was shown that a molecule like TSPP has a "dark" effect as well as one that is mediated by absorption of light.[2] Therefore, our research activity has focused on determining the mechanistic damage produced by irradiation of porphyrins non-covalently bound to tubulin. We believe that the mechanistic explanation of such effects holds great potential for the further application of PAM-mediated protein photodamage in the biomedical and technological fields.

The project has been carried out using a combination of optical techniques and molecular simulations in order to provide a thorough mechanistic model that uses the computational approach to help interpret the experimental data. The experimental techniques employed in this study are traditional biophysical techniques used in the investigation of protein-ligand interactions and the investigation of protein conformation. Techniques include fluorescence spectroscopy, fluorescence decay, and Circular Dichroism Spectroscopy (CD). The computational simulation for the moment is limited to the docking of porphyrins to proteins, used to establish the more favorable binding sites. The computational portion of the study is paramount as only by establishing the location of the binding site with a high degree of certainty, one can interpret their induced protein photodamage which is likely to be initially localized at the binding site.

# 2. RESEARCH ACTIVITY AND RESULTS

## 2.1. Binding of porphyrins to globular proteins

Prior to this study, we had already established the binding parameters of protoporphyrin IX (PPIX) to BLG and the role of the pH of the solution as modulator for the binding. The project allowed us to obtain information on the binding of tetra-phenyl-sulfonato porphyrin (TPPS) to BLG, as well as study the binding of the two porphyrins on tubulin.

## 2.2. Binding of TPPS to BLG

*Absorption spectroscopy.* At all pH values the addition of BLGA to a stock solution of TPPS4- produces a small bathochromic shift of the Soret band (from 413 nm to 416 nm) and simultaneous hypochromicity (Figure 2).

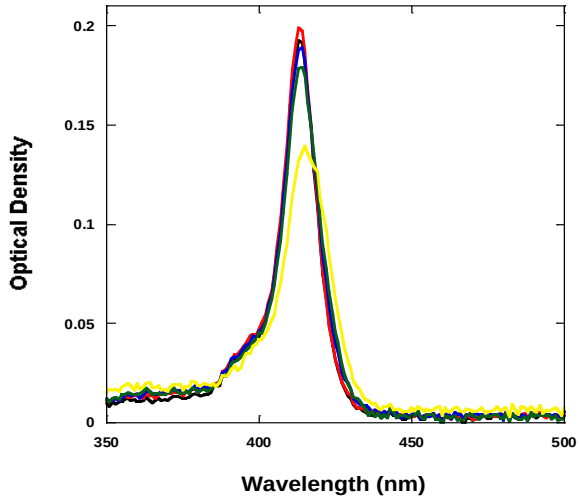


**Figure 2 Absorption spectrum of TPPS**

The same effect occurs at every pH probed in this study. In agreement with what was suggested by previous results[11] there is no evidence for the formation of J-aggregates of $TPPS^{4-}$ (appearance of a band near 490 nm) either before or after the addition of the protein. Moreover, there is no clear shift of the Q-bands induced by the presence of BLGA.[12]

*Fluorescence of $TPPS^{4-}$ bound to BLGA.* At all pH values the addition of BLGA prompts a shift of the emission maximum to longer wavelengths (Figure 3A and 3B). Such shift is larger (> 4nm) and occurs much earlier than the one observed in absorption (Figure 2). The red-shift is more pronounced at higher pH values (Figure 3(C)). However, Figures 3(A) and 3(B) also show that the normalized and corrected intensity of the $TPPS^{4-}$ emission, changes only slightly in the presence of BLGA.

Such small change would not allow the applications of fluorescence intensity methods to establish the amount of bound porphyrin.[13,14] Therefore, the contribution of free and bound porphyrin to the emission spectrum must be retrieved via Gaussian analysis of the emission spectra with equation 1 (Figure 1).

$$I(\lambda) = [L]_f C \sum_j \Phi_{f,j} G_{f,j}(\lambda) + [L]_b \alpha \sum_j \Phi_{b,j} G_{b,j}(\lambda) \qquad (1)$$

Here, $C$ is an instrumental constant, $[L]_f$ and $[L]_b$ are the concentrations of free and bound porphyrin, $\Phi_j$ is the respective fluorescence quantum yield and $G_j(\lambda)$ is the Gaussian of the *j-th* component to the spectrum centered at wavelength, $\lambda_j$ for free and bound porphyrin respectively, and $\alpha$ is the fraction of quenching.

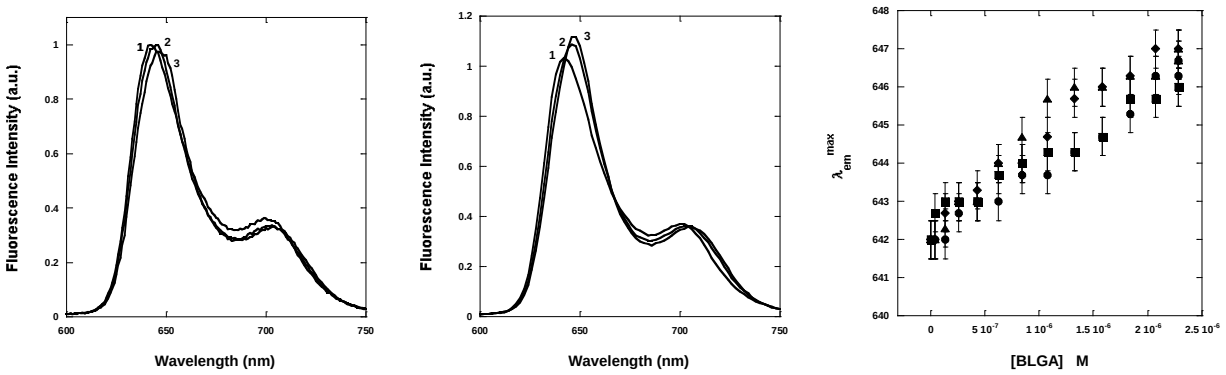


**Figure 3 Fluorescence spectra of $TPPS^{4-}$ upon addition of BLGA.** 1 **[BLGA] = 0 µM;** 2 **[BLGA] = 1.33 µM;** 3 **[BLGA] = 2.07 µM. (A) pH 6; (B) pH 9. The spectra show the red-shift of the emission upon binding to the protein. The spectra also show little change of the emission intensity. (C) Position of the emission maximum of $TPPS^{4-}$ as a function of the concentration of BLGA. (●) = pH 6, (■) = pH 7, (◆) = pH 8, (▲) = pH 9. The red-shift occurs nearly at the same rate at all pH values.**

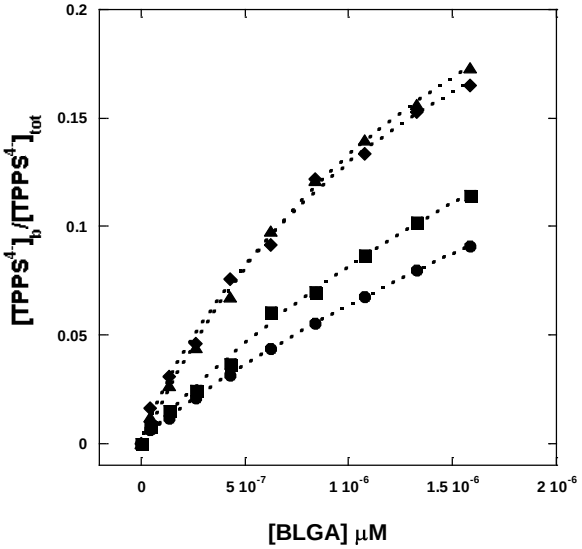


**Figure 4 Plot and fitting of bound/total $TPPS^{4-}$ according to equation 3. (●) = pH 6, (■) = pH 7, (◆) = pH 8, (▲) = pH 9**

The plots of $[TPPS^{4-}]_b/[TPPS^{4-}]_{Tot}$ vs. [BLGA] obtained from the Gaussian fitting show the relative increase of the fraction of bound porphyrin (Figure 4). The range of protein and TPPS concentration has to be kept relatively low because of the restriction on the optical density (O.D.) of the samples imposed by the fluorescence method; in particular, signal linearity requirements impose that the O.D. at the excitation wavelength be < 0.2. Nevertheless, analysis of the isotherms in Figure 4 with equation 2, yields an estimate of the binding constant, *K*, the coefficient *n*, and the factor $\gamma$, which are summarized in Table 1. The data show that the binding constant increases by approximately 20% with increasing pH. The value of *n* remains < 1 at all pH values indicating a negative correlation, and decreases by about 16% as the pH increases. A student's t-test analysis reveals that differences in the value of *K* between pH are not statistically significant (p-value $\geq$ 0.2). Similarly, an analysis of the value of *n* reveals that, although its decrease with increasing pH is consistent with electrostatic surface binding of $TPPS^4$,[15] the differences in its value at various pH are not statistically significant (p-value $\geq$ 0.1). Thus we are led to conclude that that approximately 1 TPPS molecule binds to each BLGA unit and that the binding constant is approximately constant across the range of pH.

$$\frac{[Porphyrin]_b}{[Tubulin]} = \frac{\frac{nK_b}{\Phi_b}[Porphyrin]}{1+K_b[Porphyrin]} \qquad (2)$$

A large increase with the pH occurs in the value of $\gamma$ (Table 1), where $\gamma$ is given by the ratio of $nK_b/\Phi_b$. This factor depends on the emission quantum yields for bound and free $TPPS^{4-}$. Individual quantum yields for free and bound porphyrins at various pH values could not be experimentally calculated and are not available from the literature; therefore, our fitting only indicates that the large change in the binding isotherm of Figure 4 is due to changes of the emission quantum yields of the free and bound porphyrin at the different pH values.

**Table 1 Binding parameters obtained from the fluorescence of $TPPS^{4-}$ using Gaussian fitting and equation 2**

| | $\gamma$ | $K$ x $10^{-5}$ ($M^{-1}$) | $n$ |
|---|---|---|---|
| pH 6 | 0.67± 0.12 | 0.63 ± 0.14 | 0.85 ± 0.04 |
| pH 7 | 0.72 ± 0.14 | 0.75 ± 0.17 | 0.86 ± 0.06 |
| pH 8 | 0.85 ± 0.13 | 0.76 ± 0.16 | 0.69 ± 0.10 |
| pH 9 | 0.95 ± 0.17 | 0.78 ± 0.18 | 0.71 ± 0.08 |

*Quenching of BLGA by TPPS*. Each BLGA monomer has two Trp residues, thus each BLGA dimer has potentially four Trp residues that can be quenched. The contribution of each residue to BLGA fluorescence is still under debate but some convincing studies suggested that only Trp19 at the bottom of the interior barrel contributes to the fluorescence of the protein.[16,17] We therefore used equation 3 to assess whether the BLGA/$TPPS^{4-}$ complex retains some residual fluorescence. The results show (Figure 5A) that the porphyrin quenches 80-100% of the monomer fluorescence and that this ratio is basically independent of the pH of the solutions as seen in Table 2.

$$\frac{I}{I_0} = 1 - \alpha \frac{[Porphyrin]}{[Tubulin]} \qquad (3)$$

Fluorescence spectra of BLGA as a function of added porphyrins (supplemental material) show that the decrease of protein fluorescence is not accompanied by a shift in its emission maximum. The values of the binding constants retrieved from S-V plots (Figure 5(B) and Table 2) are numerically in good agreement with the ones retrieved from $TPPS^{4-}$ fluorescence (Table 1) and they do not appear to be pH-dependent.

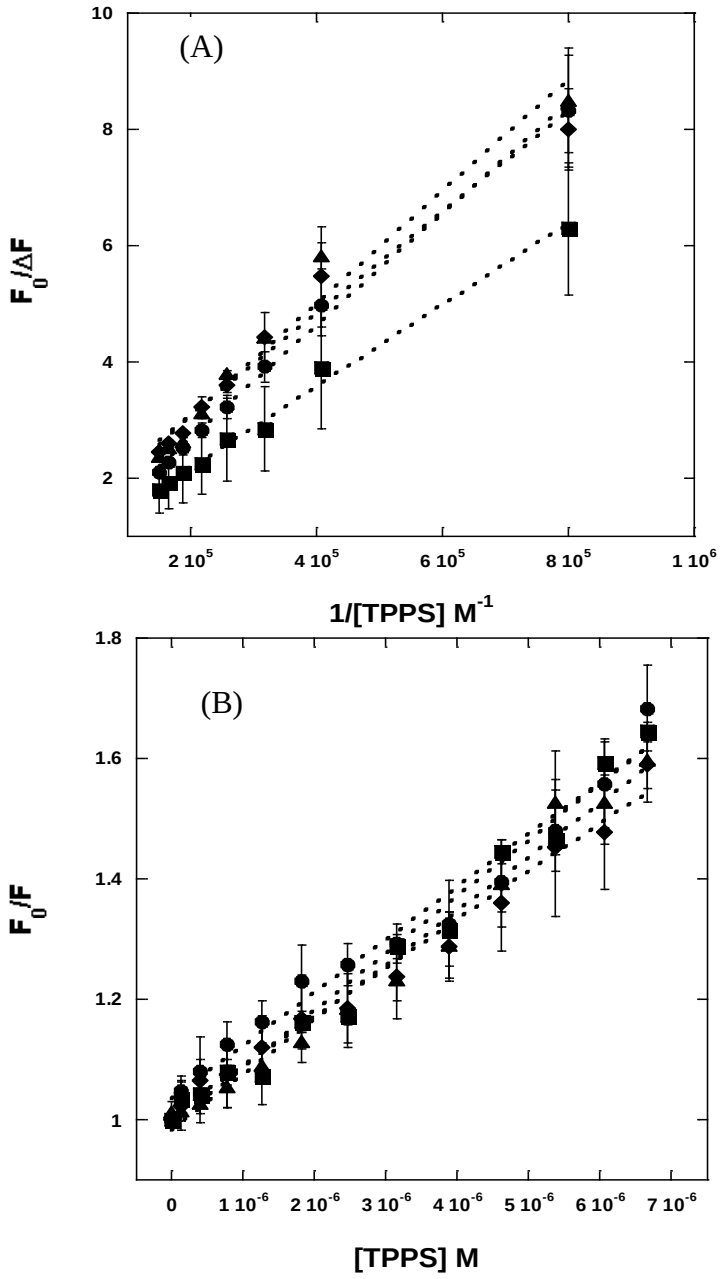


**Figure 5 (A) Plot $F_0/\Delta F$ according to equation 10 (model of fractional quenching of Lehrer[18]). (B) Stern-Volmer plot of BLGA fluorescence corrected according to equation 11. (●) = pH 6, (■) = pH 7, (◆) = pH 8, (▲) = pH 9**

**Table 2 BLGA fluorescence quenching. Fraction of quenched fluorescence and binding constant**

| | ***α*** ***(fractional quenching)*** | ***K* x $10^{-5}$ ($M^{-1}$)** |
|---|---|---|
| pH 6 | 0.89 ± 0.09 | 1.56 ± 0.33 |
| pH 7 | 1.10 ± 0.05 | 1.10 ± 0.25 |
| pH 8 | 0.91 ± 0.03 | 1.37 ± 0.29 |
| pH 9 | 0.96 ± 0.08 | 1.14 ± 0.18 |

*Fluorescence resonance energy transfer FRET*. Steady state and fluorescence lifetime experiments rule out any significant FRET between the Trp residue and the bound $TPPS^{4-}$. Excitation of Trp residues does not produce emission by the ligands and, likewise, excitation spectra recorded at the maximum of the emission wavelength of the porphyrin do not show any contribution from Trp. Fluorescence decay experiments also reveal that there is no change in BLGA emission lifetime upon addition of $TPPS^{4-}$. Such result is also in strong support of the occurrence of static quenching due to binding of the porphyrin to the protein. Lack of FRET is consistent with what had been observed in other systems[19,20] and is a direct consequence of the very small overlap between the emission spectrum of BLGA and the absorption spectrum of $TPPS^{4-}$.

*Circular Dichroism.* At all pH values, CD experiments in the region of the Soret band did not show any optical activity of $TPPS^{4-}$ which indicates that binding to BLGA does not distort the structure of the porphyrin ring. At the same time the binding of the porphyrin did not produce any change in the dichroic signal of BLGA either in the region of the aromatic amino acids (260-320 nm) or in the region of the amide (180-250 nm).

*Effects of urea*. In order to probe whether the porphyrin binds to sites at the monomer/monomer interface we studied the effects of the addition of urea to solutions containing the BLGA/$TPPS^{4-}$ non-covalent complex. It is known that within a certain range of urea concentrations, which depends on the pH of the solution,[21] BLGA dimers dissociate without any appreciable change in the tertiary structure of the individual monomers.[21] Thus if $TPPS^{4-}$ binds to the dimer at the interface between the two monomers, the addition of urea may cause the porphyrin to return in solution upon dissociation of the dimers.

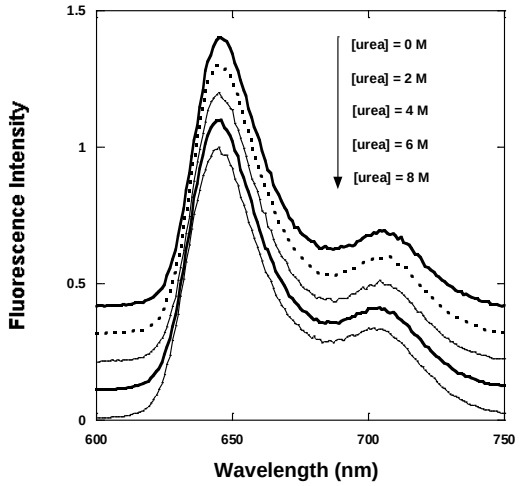


**Figure 6 Fluorescence of $TPPS^{4-}$ in the protein/porphyrin complex as a function of urea concentration. The spectra are normalized and offset with respect to each other to show that the emission maximum of bound $TPPS^{4-}$ is not affected by the addition of up to 8 M urea**

This in turn would cause the emission maximum of the porphyrin to blue-shift towards the position of free $TPPS^{4-}$. Our results, however, show (Figure 6) that addition of urea up to 8 M (a concentration where urea is known to partially unfold the monomeric form of BLGA [21,22]) does not cause any shift of fluorescence of BLGA-bound $TPPS^{4-}$. Addition of the same aliquots of urea to solutions containing only TPPS produced only a slight (2 nm) red-shift of the emission of the porphyrin, probably due to the sequestration of water molecules by urea. Since the red-shift resulting from binding to BLG is 7 nm, the lack of blue-shift of BLG-bound TPPS upon addition of urea indicates that $TPPS^{4-}$ remains attached to the protein even when this is partially unfolded. The dissociation and unfolding of BLGA at increasing urea concentration was probed by the red-shift and the increase in intensity of the intrinsic fluorescence of the protein[16]. The comparison of urea-induced denaturation of BLGA alone and BLGA in the protein/porphyrin complex shows that the presence of bound $TPPS^{4-}$ stabilizes BLGA, as the sigmoidal transition to the unfolded state appears to be delayed (Figures 7(A) and 7(B)). Calculation of $\Delta G^0_{DCU}$ and *m* produces the values shown in Table 3.

**Table 3 Thermodynamic parameters for the urea-induced unfolding of BLGA in the complex with $TPPS^{4-}$ and alone at different pH values**

| | ***m*** **BLGA/$TPPS^{4-}$ complex** | ***m*** **BLGA alone** | **$\Delta G^0_{DCU}$ (kJ/mol) BLGA/$TPPS^{4-}$ complex** | **$\Delta G^0_{DCU}$ (kJ/mol) BLGA alone** |
|---|---|---|---|---|
| pH 6 | 6.38 ± 0.52 | 4.44 ± 0.91 | 74.4 ± 4.1 | 51.1 ± 5.1 |
| pH 7 | 4.46 ± 0.78 | 2.86 ± 0.40 | 53.3 ± 4.5 | 38.0 ± 4.3 |
| pH 8 | 3.38 ± 0.42 | 2.79 ± 0.27 | 45.3 ± 4.3 | 35.8 ± 4.5 |
| pH 9 | 2.53 ± 0.61 | 2.53 ± 0.22 | 40.1 ± 4.0 | 34.8 ± 5.0 |

By comparison with the data obtained in the absence of $TPPS^{4-}$ it can be seen that while the denaturant index, *m*, remains virtually unchanged, $\Delta G^0_{DCU}$ of the BLGA/porphyrin complex increases, at all pH values. The increased stability against denaturation induced by binding of $TPPS^{4-}$ is larger at smaller pH (Figure 7C).

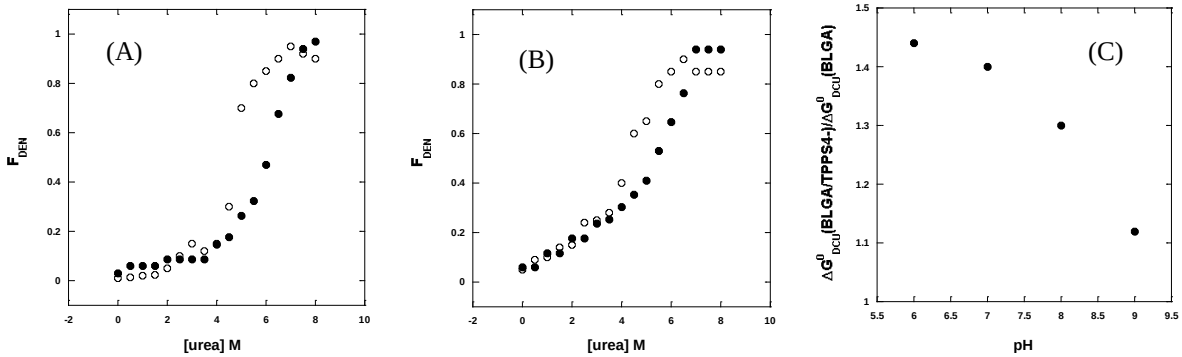


**Figure 7 Denaturation curves calculated using the wavelength of the emission maximum as the indicator of denaturation. (A) pH 7: (●) = BLGA/$TPPS^{4-}$ complex, (○) = BLGA alone; (B) pH 9: (●) = BLGA/$TPPS^{4-}$ complex, (○) = BLGA alone. The data are representative of the trend at the other pH values. (C) Relative increase of $\Delta G_{DCU}$ induced by the presence of bound $TPPS^{4-}$ as a function of pH**

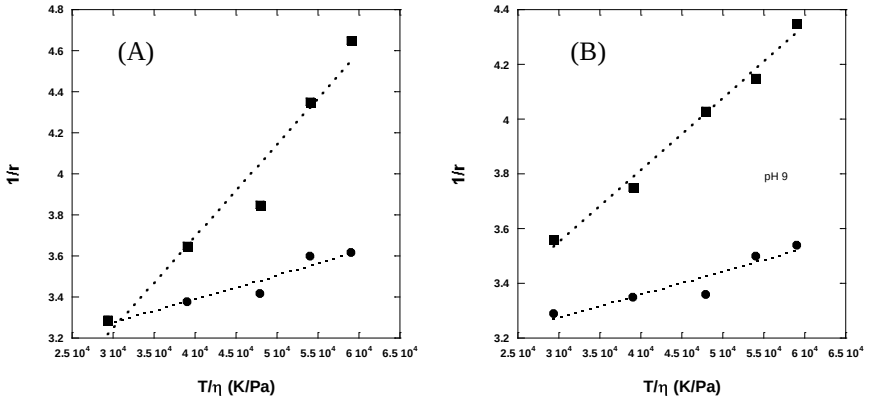


**Figure 8 Perrin plots of the steady state fluorescence anisotropy. (A) pH 6: (●) = BLGA/$TPPS^{4-}$ complex, (■) = $TPPS^{4-}$ alone; (B) pH 9: (●) = BLGA/$TPPS^{4-}$ complex, (■) = $TPPS^{4-}$ alone. The data are representative of the trend at the other pH values and show a larger slope for TPPS alone than for the porphyrin bound to the proteins**

*Fluorescence Anisotropy***.** Perrin plots are linear and show, as expected, a steeper slope for free TPPS than for the BLGA/TPPS complex at all pH (Figure 8A and 8B). From the slope of the plot and upon measurements of free and bound TPPS fluorescence lifetime (9.8 ns and 11 ns respectively) we estimated the radius of the free ligand to be < 1 nm and the radius of the complex to be 2.5-3 nm. The radius of the BLGA/TPPS complex is in excellent agreement with

the size of the BLGA dimer reported by others.[23,24] This in turn confirms that in the pH and concentration range investigated, binding of $TPPS^{4-}$ does not induce aggregation of BLGA.

*Docking Simulations.* A survey of the BLGA dimer structure (PDB file 1BEB.pdb) provides several potential binding sites for $TPPS^{4-}$. There are several Lys and Arg residues on the surface as well as in the grove formed between the 3-turn helix and the outside of the β-barrel.[25-27] In addition, we investigated the docking at intradimeric sites on the side of the 3-turn helices as well as on the side of the aperture of the barrel.[28] We attempted the docking to all these locations by approaching $TPPS^{4-}$ at different orientations to each site. Our results show that there is no stable binding configuration for either the interior of the β-barrel or the outside grove. In addition, docking at the monomer-monomer interface did not yield stable binding configurations.

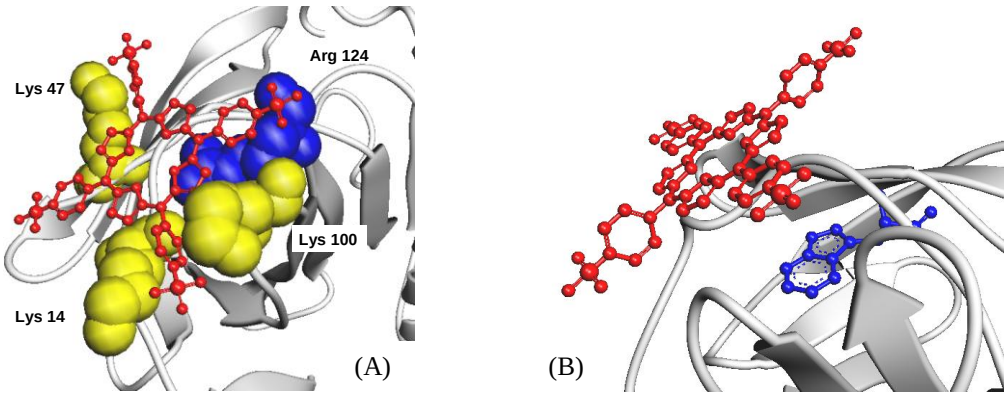


**Figure 9 Simulation of the docking of $TPPS^{4-}$ to BLGA. (Left) The most stable docking configuration produces $TPPS^{4-}$ (red) laying flat on the surface of BLGA with its four $SO_3^-$ groups interacting with Lys (yellow) and Arg (blue) positively charged residues. (Right) Different view of the same binding site which shows that $TPPS^{4-}$ (red) is < 8 Å away from the indole ring of Trp19 (blue)**

Our docking computation revealed that the most likely binding site for $TPPS^{4-}$ is on the surface of BLGA at a location which involves a near interdigitation of three of the four $SO_3^-$ groups of $TPPS^{4-}$ and the positively charged side chains of Lys14, Lys47, Lys100 and Arg124 (Figure 9A). This location also places the ligand in proximity (~ 7.2 Å) of the fluorescent Trp19 residue (Figure 9B) which would explain the static quenching produced by the binding of $TPPS^{4-}$ to BLGA. Thus, the computed binding site involves regions that include the N-terminus, the B-strand, the FG-loop, and the loop between strand I and the 3-turn α-helix.[26,27] Because of the large number of surface Arg and Lys it is likely that other surface regions may also be docking sites to the porphyrin.

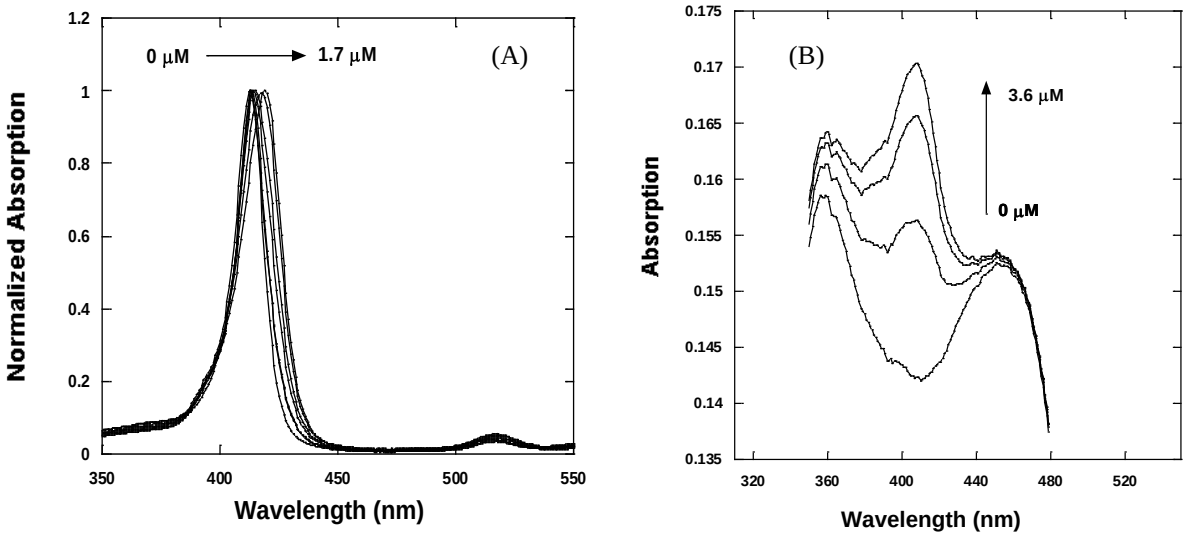


**Figure 10 (*A*) Absorption spectra of TSPP upon addition of tubulin. The arrow indicates the red-shift of absorption from 413 nm to 420 nm. (B) Absorption spectra of PPIX upon addition of tubulin. The peak of monomeric (bound) PPIX appears and increases (arrow) over the broad, poorly structured spectrum of PPIX in buffer**

## 2.3. Binding of Porphyrins to Tubulin

*Absorption spectroscopy of binding porphyrins.* The addition of increasing aliquots of tubulin to the aqueous solution produced a red shift of the absorption maximum of TSPP (Figure 10A), and the appearance of a peak at 405 nm over the unstructured spectrum of PPIX (Figure 10B). This is in agreement with what observed in other studies of porphyrin/protein non-covalent binding and has been explained as (i) binding of porphyrin macrocycles to non-aqueous sites[29,30] and/or (ii) monodispersion[19,31]. Figure 10(A) also shows that binding of TSPP to tubulin does not induce formation of J-aggregates as observed in other studies.[11]

*Porphyrin Fluorescence.* Addition of tubulin to the solution causes the emission of TSPP or PPIX to increase in intensity and shift to longer wavelengths. The maximum of TSPP shifts from 642 nm to 649 nm and the maximum of PPIX shifts from 620 nm to 631 nm. The Gaussian fitting of the emission spectra shows that, as more tubulin is added to solutions containing porphyrin, the peak of bound porphyrin increases relatively to the one of free porphyrin. The areas of the Gaussians associated with the bound and free porphyrin yield the value of $\Phi_b[L]_b$ and $\Phi_f[L]_f$ respectively.

Upon substitutions of the values and fitting with the following equation

$$\frac{[Porphyrin]_b}{[Tubulin]} = \frac{\frac{nK_b}{\Phi_b}[Porphyrin]}{1+K_b[Porphyrin]} \qquad (4)$$

We retrieved values (Figure 11) of $K_b$ = 2.19 (± 0.64) x $10^5$ $M^{-1}$ and $K_b$ = 2.22 (± 0.29) x $10^6$ $M^{-1}$ for PPIX and TSPP respectively. From the values of $K_b$ the ratio $n/\Phi_b$ was calculated as 9.8 (± 2.1) for PPIX and 3.8 (± 0.9) for TSPP.

By fitting the data one can then independently obtain an estimate for $n$ and $\Phi_b$. The analysis with the equation above yields $n$ = 1.3 ± 0.5 and $n$ = 1.2 ± 0.4 for PPIX and TSPP respectively. From the values of $n$, $\Phi_b$ was estimated at 0.13 for PPIX and 0.26 for TSPP.

*Quenching of tubulin fluorescence.* Addition of TSPP or PPIX to tubulin solutions quenches the intrinsic fluorescence of the protein. The effect is accompanied by a slight blue shift of the protein emission maximum which is smaller for PPIX ($\Delta\lambda$ = 2 nm) than for TSPP ($\Delta\lambda$ = 4 nm). Because of the presence of multiple Trp residues in tubulin, fluorescence analysis requires that we determine the fraction of tubulin fluorescence that is quenched by porphyrin.

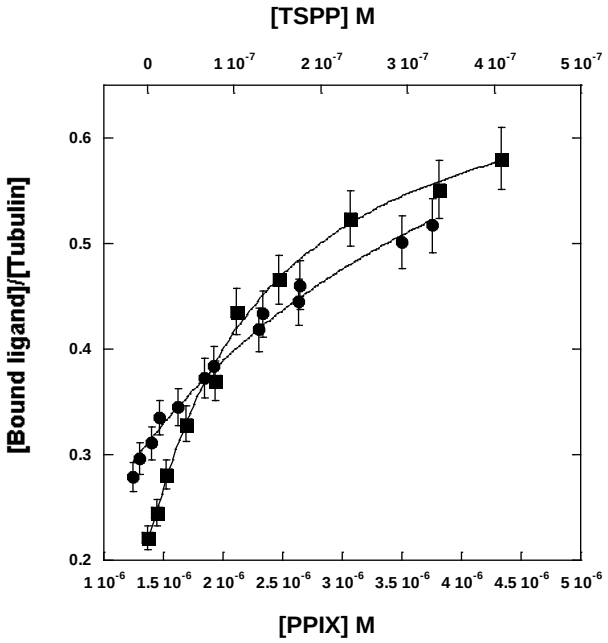


**Figure 11 Binding curves obtained from Gaussian fitting (equation 7). (●) PPIX; (■) TSPP. Note that the scale of the x-axis is different for the two porphyrins**

*Fractional fluorescence change.* The fraction of quenched tubulin fluorescence can be estimated using equation 3. The linear regression yielded values of $\alpha$ = 0.10 ± 0.02 and $\alpha$ = 0.14 ± 0.08 for PPIX and TSPP respectively. The values are similar to the ones that were obtained using the crude extrapolation of the reciprocal plot ($F_0/\Delta F$ vs $1/[Q]$) proposed by Lehrer for collisional quenching ($\alpha$ = 0.11 ± 0.02 and $\alpha$ = 0.25 ± 0.11).

*Stern-Volmer.* The S-V plots show an upward curvature for quenching with either porphyrin (Figure 6). This may suggest the overlap of a dynamic and a static quenching component which could be justified by the presence of two exposed Trp residues (Trp 346α and Trp 407β). However, since the fluorescence lifetime of tubulin does not change under these conditions (see

below), a dynamic component to the quenching was ruled out. Therefore, we assumed that the quenching was purely static and at low porphyrin concentration could be described by an equation linear with the concentration of the quencher (Stern-Volmer plot). The linear limit was different for PPIX (< 3 μM) and TSPP (< 1 μM) and the linear regression yielded $K_b$ = 1.41 (± 0.29) x $10^5$ $M^{-1}$ for PPIX and $K_b$ = 7.20 (± 0.47) x $10^5$ $M^{-1}$ for TSPP.

## 2.4 Time resolved fluorescence

*Tubulin.* The decay of tubulin intrinsic fluorescence reveals a non-exponential decay with three components summarized in Table 4. Because of the large number of Trp residues a complex multi-exponential decay is expected.[32]

**Table 4 Decay parameters of tubulin fluorescence with and without porphyrin**

| | $\alpha_1$ | $\tau_1$ | $\alpha_2$ | $\tau_2$ | $\alpha_3$ | $\alpha_1$ |
|---|---|---|---|---|---|---|
| *Tubulin* | 0.11 ± 0.08 | 0.63 ± 0.28 | 0.36 ± 0.07 | 2.41 ± 0.31 | 0.53 ± 0.08 | 5.30 ± 0.47 |
| *Tubulin+PPIX* | 0.15 ± 0.07 | 0.54 ± 0.29 | 0.32 ± 0.10 | 2.29 ± 0.31 | 0.53 ± 0.11 | 5.21 ± 0.68 |
| *Tubulin+TSPP* | 0.13 ± 0.08 | 0.58 ± 0.28 | 0.39 ± 0.12 | 2.34 ± 0.31 | 0.48 ± 0.11 | 5.26 ± 0.71 |

The relative contribution of the long-lived component (τ > 5 ns) suggests that the more exposed Trp residues may contribute to the majority of the protein fluorescence.[33-35] We did not attempt to separate the contribution of the single Trp residues.

*Porphyrins*. The fluorescence decay of TSPP and PPIX are affected by the binding to tubulin in agreement with previous observations.[11,36,37] PPIX fluorescence decay, which is bi-exponential in aqueous solution, becomes virtually monoexponential when the porphyrin binds tubulin (Table 3). The relative amplitude of the short-lived component is quite small for the free ligand (6%), however, upon binding of tubulin its contribution decreases to ≈ 1%. The lifetime of the dominant component increases by approximately 1 ns upon binding to tubulin.

**Table 5 Fluorescence lifetime of TSPP and PPIX with tubulin (Excitation 405nm)**

| | $\alpha_1$ | $\tau_1$ | $\alpha_2$ | $\tau_2$ |
|---|---|---|---|---|
| TSPP | 0.02 ± 0.02 | 1.60 ± 0.12 | 0.98 ± 0.04 | 9.90 ± 0.11 |
| TSPP + tubulin | < 0.01 | < 1 ns | 0.98 ± 0.03 | 11.7 ± 0.18 |
| PPIX | 0.06 ± 0.02 | 1.57 ± 0.33 | 0.94 ± 0.05 | 14.3 ± 0.15 |
| PPIX + tubulin | < 0.01 | < 1 ns | 0.98 ± 0.05 | 16.5 ± 0.14 |

The fluorescence lifetime of TSPP is monoexponential in aqueous solution and after binding to tubulin. However the lifetime lengthens from 9.9 ns to 11.7 ns (Table 3).

*Fluorescence decay of tubulin in the presence of porphyrins.* The addition of either porphyrin does not change the individual components or the average lifetime of tubulin fluorescence (Table 5). This supports our assumption that the fluorescence quenching of the protein is due entirely to static quenching caused by binding. It also appears to be in agreement with quenching of only a small portion of the Trp residues in tubulin.

*FRET.* Table 5 clearly indicates that addition of porphyrins does not affect the fluorescence decay of tubulin, thus suggesting the absence of FRET between Trp residues and porphyrins. Additional support is provided by steady-state emission and excitation spectroscopy. Excitation of tubulin at 280 nm in the presence of PPIX or TSPP does not produce an increase of the porphyrin emission intensity. Likewise, the excitation spectrum of porphyrin-protein mixtures does not show any increase of tubulin contribution when the emission wavelength was fixed to the value of the bound porphyrin. In fact, excitation spectra of solutions containing only tubulin and no porphyrin, recorded with emission wavelength at 631 nm or 649 nm, show a contribution of the protein. Since the protein fluorescence does not contribute at such long wavelength, we explain this as an artifact due to the fact that the range of emission wavelengths for the porphyrins (630-650 nm) overlaps with the first harmonic of the emission of the protein (315-325 nm), thus causing the appearance of the tubulin excitation spectrum.

*Polymerization of tubulin.* We investigated whether the fluorescence effects observed could be attributed to polymerization of tubulin during the fluorescence experiments. To do so we carried out scattering experiments (turbidity assay [13,38]) under the same conditions of temperature and buffer as used for the fluorescence experiments. As expected, by operating at room temperature and in simple phosphate buffered solution the polymerization of tubulin was inhibited in the time scale of a typical fluorescence experiment (2-3 hrs) even at much higher tubulin concentration (5 μM). The addition of TSPP and PPIX did not induce any polymerization (Figure 12). We thus ruled out that our results were affected by binding of porphyrin to polymerized tubulin.

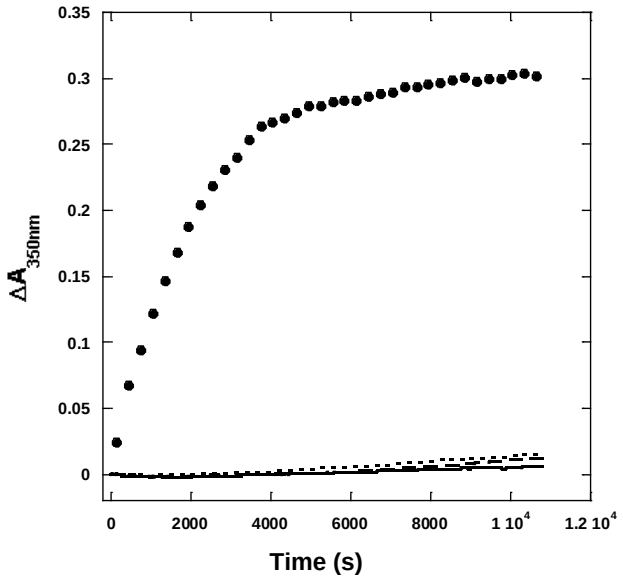


**Figure 12 Polymerization of tubulin. The figure shows that under the condition of buffer and temperature of the fluorescence experiments, 5 µM tubulin alone (—) as well as in the presence of 2.5 µM PPIX (•••) or 2.5 µM TSPP (— — —) does not polymerize. Under the same conditions the presence of 2.5 µM taxol (●) does instead induce polymerization**

*Docking simulation***.** Docking of PPIX yielded several possible binding configurations. The one characterized by the lower minimum was partly overlapped to the Taxol site (-11.9 kcal/mol). This site did not produce proximity to any Trp residue, the closest being Trp21 of the β-monomer located > 20 Å away from the center of the porphyrin ring. The configuration that produced the best combination of minimum energy (-11.2 kcal/mol) and proximity to Trp residues is a site partly overlapped with the nucleotide site on the β-monomer. Such site brings PPIX and Trp407 in close contact (Figure 13A). Other sites in the proximity of Trp residues or near the location of the colchicine binding site, produced stable configurations with much smaller energy minima (- 4.5 kcal/mol < ΔG < -9.0 kcal/mol). Since fluorescence experiments suggest that there are two porphyrins bound to each tubulin dimer one of these sites, not shown in Figure 13, could represent the second docking location. Docking of TSPP yielded fewer possible binding configurations than PPIX, likely because of the four negatively charged $SO_3^-$ groups symmetrically distributed around the ring. The one characterized by the lower minimum (-10.6 kcal/mol) is located between the taxol site and the GTP/GDP site on the β-monomer. This configuration also brings the center of the TSPP ring ~ 11 Å from the N1 atom of the indole ring of Trp21 (Figure 13B). Also at this site one of the $SO_3^-$ groups is located equidistant (~ 5 Å) from two basic residues: His229 and Lys19 (Figure 13C). Docking of TSPP to the site of taxol, colchicines, vinblastine, as well as sites in proximity of other Trp residues resulted in either no energy minimization or configuration with shallower minima (-5.0 kcal/mol < ΔG < -6.8 kcal/mol). However because fluorescence data indicate the binding of a second TSPP molecule, it is likely that one of these site would also be occupied.

An interesting observation is that in nearly all docking configurations, such as the one shown in Figure 10, the indole ring of the most proximal Trp residues and the ring of the porphyrins were nearly at a 90˚ angle, thus independently supporting the absence of FRET between Trp residues and porphyrins [39]. More detailed docking studies are ongoing and may shed further light on the location of the binding sites for PPIX and TSPP and the resulting intermolecular interactions.

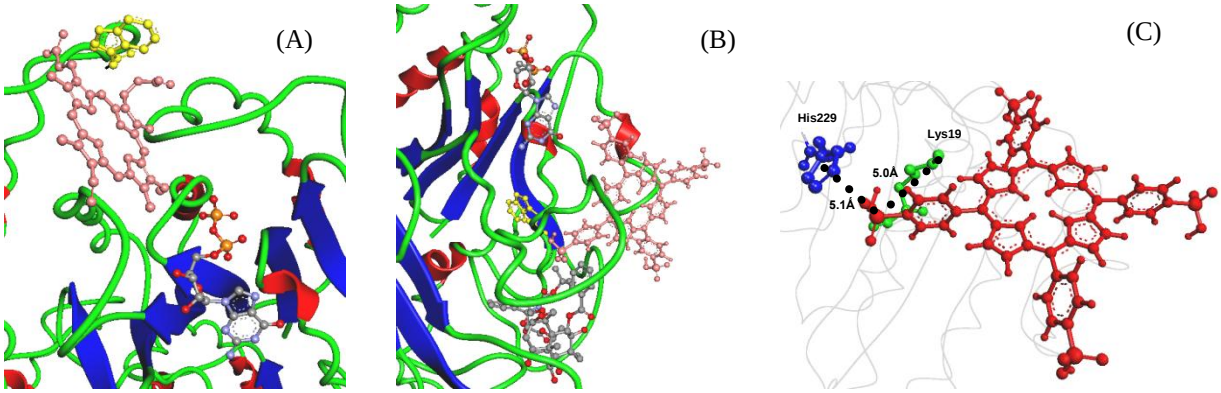


**Figure 13 (A) Molecular simulations using ArgusLab show that the location of the most stable binding site for PPIX (pink) is located proximal, but not overlapped, to the nucleotide (CPK color) site and places PPIX in contact with Trp407 in the β-monomer (yellow). (B) The site of TSPP (pink) places it between the location of GTP and taxol (both in CPK colors) and at ~ 8 Å from Trp21 in the β-monomer (yellow). In both (A) and (B) the indole ring is nearly perpendicular to the porphyrin ring. (C) One of the $SO_3^-$ groups of TSPP (red) is in proximity and equidistant with Lys19 (green) and His229 (blue)**

# 3 PHOTODAMAGE OF GLOBULAR PROTEINS MEDIATED BY PORPHYRINS IRRADIATION

*Irradiation dependence of TPPS and BLG absorption*. Irradiation of the TPPS/BLG complex leads to bleaching of the protein (279 nm) and the porphyrin (413 nm). The decrease at 279 nm is accompanied by the increase of a broad shoulder near 320 nm (Figure 14A and B). At pH ≥ 8 the Soret band of TPPS shifts by ~ 5 nm to longer wavelengths. Since the concentration of TPPS was low (~ 1μM) the Q-bands were not clearly visible, therefore the effects of irradiation in this region was investigated using fluorescence excitation spectra but they did not reveal any additional information other than a shift of the lowest energy Q(0,1) band (supplemental material). The relative bleaching of BLG and TPPS is larger for increasing pH values (equal amount of photon energy density ($J/cm^2$) deposited in the sample). The increase of the shoulder at 320 nm is twice as large at pH 8 and 9 than at pH 6 (Figure 14B). At alkaline pH but not at pH 6 and 7, the bleaching of TPPS is accompanied by a shift in the Soret band (Figure 14B).

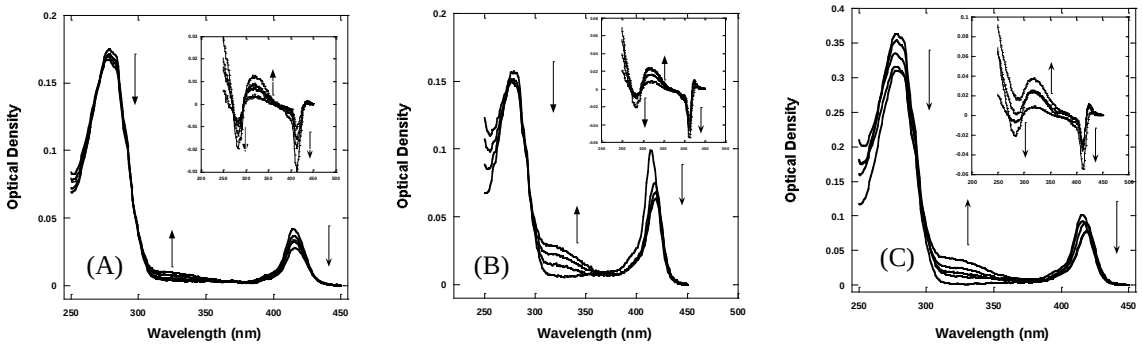


**Figure 14 Absorption spectrum of the BLG/TPPS complex as a function of the irradiation energy density (0.0, 0.3, 0.6, 1.2, 3.6 J/cm$^2$). The arrows indicate the direction of the change in absorption as the irradiation increases. (A) pH 6, air-saturated solutions; (B) pH 9, air-saturated solution; (C) pH 9, $N_2$-saturated solution. The inserts shows the difference absorption spectra between the complex at increasing irradiation energy density and the non-irradiated complex. Once again the arrows in the inserts indicate the direction of the relative change in absorption as a function of the irradiation energy density at the sample. Note that at pH 9 (in air and $N_2$) the decrease of the band near 413 nm is accompanied by a red-shift. The spectra at pH 6 are also representative of the spectra at pH 7, whereas the spectra at pH 9 are representative also of the spectra at pH 8 (supplemental material)**

Deoxygenation of the BLG/TPPS solutions did not prevent bleaching of either the porphyrin or the protein, or the formation of the band at 320 nm. As Figure 14C shows, at alkaline pH (but the same applies at pH 6 and 7) the features recorded in the air-saturated samples are still present in deoxygenated samples and the extent of the relative changes observed is comparable to that for samples in air.

*Irradiation dependence of TPPS steady-state fluorescence.* The bleaching of TPPS (Figure 14) is the reason for the decrease in its emission intensity. However, at pH ≥ 8 the photobleaching is accompanied by a 5 nm shift of the Q(1',0) emission maximum to longer wavelengths (Figure 15). Such additional shift is similar, in magnitude, to the one observed in the absorption (Figure 14(B)) and excitation spectra (supplemental material). In deoxygenated samples, irradiation produce effects similar to the ones observed in the presence of oxygen in the emission spectra of the TPPS/BLG complex.

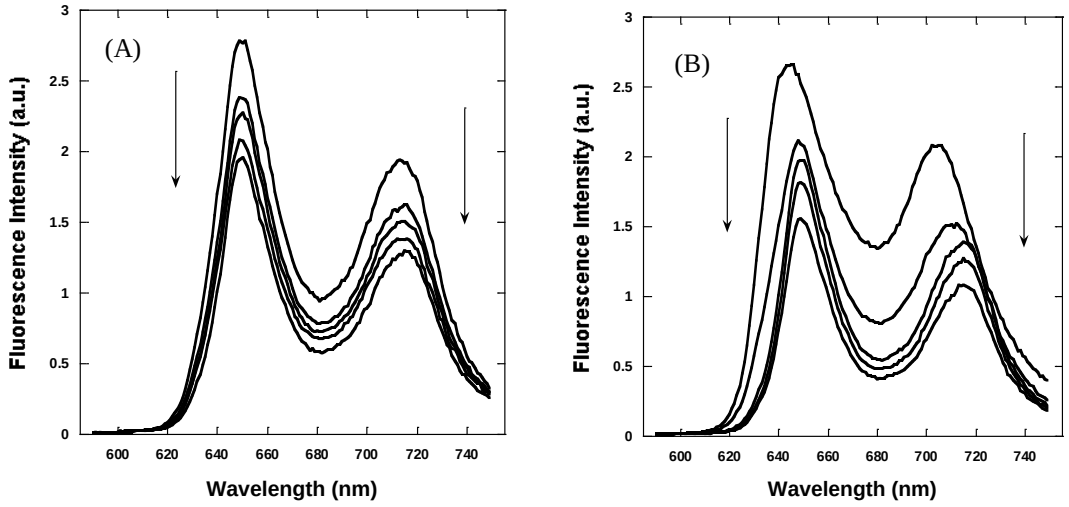


**Figure 15 Emission spectra ($\lambda_{ex}$ = 413 nm) of the porphyrin in the BLG/TPPS complex as a function of irradiation energy density (0.0, 0.3, 0.6, 1.2, 3.6 J/cm$^2$). The spectrum shows both Q'(0,0) and Q'(1,0) emission peaks and the arrows indicate the direction of the fluorescence intensity as a function of increasing irradiation energy density. (Left) pH 6, air-saturated solutions; (Right) pH 9, air-saturated solutions. The spectra at pH 6 are also representative of the spectra at pH 7, whereas the spectra at pH 9 are representative also of the spectra at pH 8**

*Irradiation dependence of UV fluorescence (BLG and products).* The irradiation-induced bleaching of BLG in absorption (Figure 14) is responsible for the decrease in the emission intensity of the protein in the TPPS/BLG complex. However, at pH ≥ 8 the decrease in intensity is accompanied by a very slight red-shift (~ 2nm) in the emission maximum which may indicate small changes around the Trp residues.

We investigated the emission properties associated with the irradiation-induced 320 nm shoulder (Figure 14). Excitation of this band produces a broad and weak emission centered near 408 nm (Figure 16A and B). The low intensity of such band is due to a combination of the small O.D. and, possibly, a smaller fluorescence quantum yield of the emitting molecule. However as, Figure 4 shows, in agreement with absorption (Figure 14) the emission intensity of this band at alkaline pH is larger than at pH 6 and 7. The excitation spectrum associated with the 408 nm broad peak, produces a component of the protein with peak at 279 nm and a shoulder at 321 nm similar to the absorption spectrum (supplementary material).

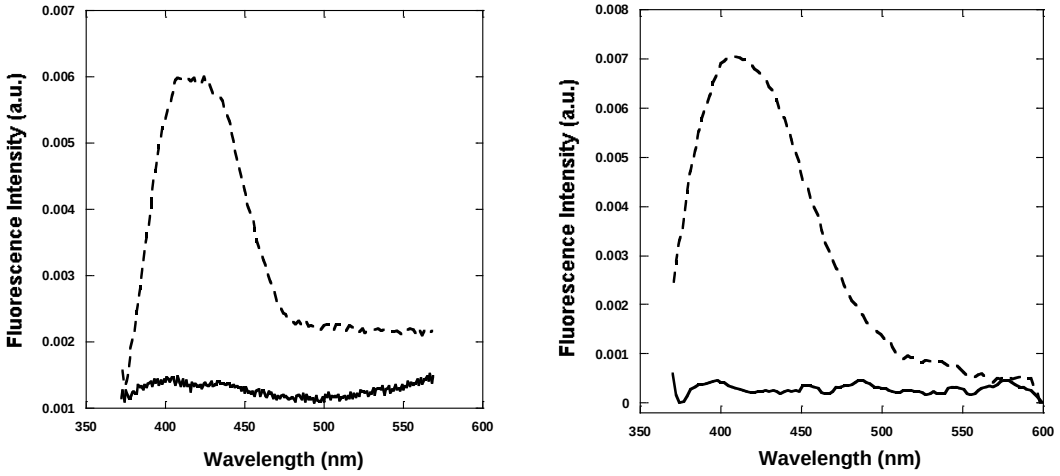


**Figure 16 Emission spectra ($\lambda_{ex}$ = 320 nm) of the non-irradiated (solid line) and irradiated (dashed line) BLG/TPPS complex. Energy density for the irradiated complex = 3.6 J/cm$^2$. (Left) pH 6, air-saturated solutions; (Right) pH 9, air-saturated solutions. The spectra at pH 6 are also representative of the spectra at pH 7, whereas the spectra at pH 9 are representative also of the spectra at pH 8**

Purging the solution with $N_2$ does not affect the steady-state emission of BLG in the complex upon laser irradiation. The protein is bleached while the maximum of the emission of BLG remains unaffected at low pH and shows the same slight red-shift at higher pH values. The emission and excitation properties of the 320 nm shoulder also remain unaffected.

*Intrinsic fluorescence lifetime of the protein in the BLG/TPPS complex (air-saturated).* Measurements of the fluorescence lifetime provide additional important information regarding the effects of irradiation. In agreement with our previous results [16], at all pH values, BLG fluorescence decay can be separated into three, pH-dependent components.

Irradiation of the samples at pH $\leq$ 7 does not affect the emission decay of the protein in the BLG/TPPS complex (Figure 17(A) and Table 1). Conversely, at pH $\geq$ 8 irradiation of the complex produces a substantial lengthening of the fluorescence decay of the protein (Figure 17B). The deconvolution of the various decay components shows that the intermediate lifetime, $\tau_2$, lengthens by 130 ps at pH 8 and 260 ps at pH 9. At the same time the longer-lived component, $\tau_3$, lengthens nearly 1 ns at both pH values (Table 1). Simultaneously, the relative amplitude of the third component, $\alpha_3$, increases at the expense of the relative amplitude of the intermediate component, $\alpha_2$ (Table 1). Conversely, the lifetime and amplitude of the sub-nanosecond component remain basically unaltered (supplemental material).

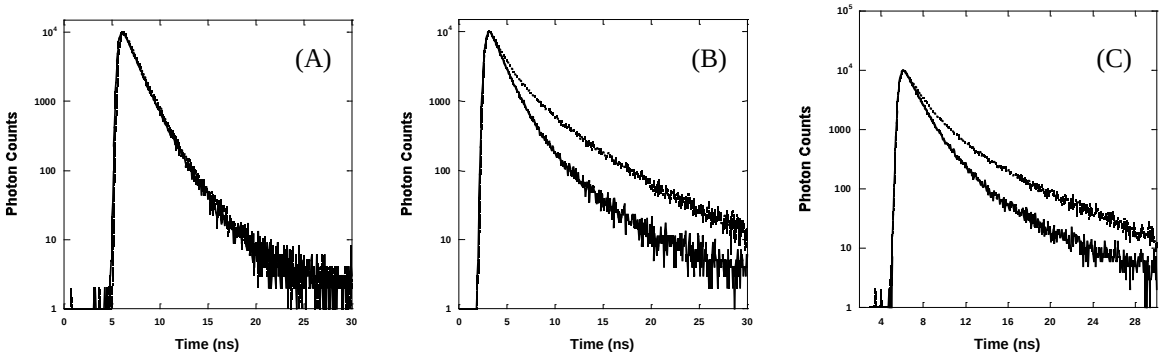


**Figure 17 Fluorescence decay of the protein in the BLG/TPPS complex. $\lambda_{ex}$ = 295 nm, $\lambda_{em}$ = 330 ± 4 nm. Solid line = non-irradiated complex; dotted line = complex irradiated with 3.6 J/cm$^2$. (A) pH 6, air-saturated solution. (B) pH 9, air-saturated solution. (C) pH 9 deoxygenated solution**

In agreement with what was already observed in absorption and steady-state emission, deoxygenation of the samples did not produce any qualitative change in the effects of irradiation, thus unequivocally suggesting that the photoinduced changes of BLG do not depend on the presence of diffusing $O_2$. As shown in Figure 17(C) irradiation of deoxygenated solutions of TPPS/BLG complex produced a lengthening of the emission decay of the protein which is comparable to the one in air (Table 6). The numerical values of the lifetimes (in particular $\tau_2$ and $\tau_3$) are larger in deoxygenated samples (for both irradiated and non-irradiated samples), according to the quenching that $O_2$ produces on the fluorescence of Trp residues in proteins.[40]

**Table 6 Fluorescence Decay parameters of BLG**

| **pH 6** | **0 (J)** | **0.3 (J/cm$^2$)** | **0.6 (J/cm$^2$)** | **1.2 (J/cm$^2$)** | **3.6 (J/cm$^2$)** |
|---|---|---|---|---|---|
| $\alpha_2$ (irr. air) | 0.71 ± 0.02 | 0.67 ± 0.03 | 0.65 ± 0.03 | 0.68 ± 0.04 | 0.67± 0.03 |
| **$\alpha_2$ (irr. $N_2$)** | **0.73 ± 0.02** | **0.76 ± 0.04** | **0.79 ± 0.03** | **0.76 ± 0.02** | **0.79± 0.04** |
| $\tau_2$ (irr. air) | 1.19 ± 0.05 | 1.17 ± 0.05 | 1.10 ± 0.11 | 1.10 ± 0.10 | 1.23± 0.11 |
| **$\tau_2$ (irr. $N_2$)** | **1.31 ± 0.06** | **1.39 ± 0.10** | **1.32 ± 0.12** | **1.33 ± 0.06** | **1.35± 0.01** |
| $\alpha_3$ (irr. air) | 0.18 ± 0.03 | 0.23 ± 0.02 | 0.25 ± 0.02 | 0.28 ± 0.02 | 0.21± 0.02 |
| **$\alpha_3$ (irr. $N_2$)** [a] | **0.20 ± 0.03** | **0.14 ± 0.03** | **0.14 ± 0.03** | **0.11 ± 0.03** | **0.11± 0.03** |
| $\tau_3$ (irr. air) [b] | 2.36 ± 0.14 | 2.27 ± 0.16 | 2.20 ± 0.21 | 2.14 ± 0.21 | 2.29± 0.22 |
| **$\tau_3$ (irr. $N_2$)** [a] | **2.48 ± 0.09** | **2.61 ± 0.13** | **2.54 ± 0.20** | **2.53 ± 0.20** | **2.52± 0.09** |
| **pH 9** | | | | | |
| $\alpha_2$ (irr. Air) | 0.69 ± 0.02 | 0.59 ± 0.03 | 0.54 ± 0.03 | 0.52 ± 0.04 | 0.49± 0.03 |
| **$\alpha_2$ (irr. $N_2$)** | **0.66 ± 0.02** | **0.62 ± 0.04** | **0.55 ± 0.03** | **0.53 ± 0.02** | **0.56± 0.04** |
| $\tau_2$ (irr. Air) | 1.37 ± 0.05 | 1.33 ± 0.05 | 1.60 ± 0.11 | 1.55 ± 0.10 | 1.63± 0.11 |
| **$\tau_2$ (irr. $N_2$)** | **1.37 ± 0.06** | **1.50 ± 0.10** | **1.59 ± 0.12** | **1.64 ± 0.06** | **1.65± 0.01** |
| $\tau_3$ (irr. air) | 0.12 ± 0.03 | 0.27 ± 0.02 | 0.28 ± 0.02 | 0.33 ± 0.02 | 0.35± 0.02 |
| **$\tau_3$ (irr. $N_2$)** | **0.11 ± 0.03** | **0.17 ± 0.03** | **0.23 ± 0.03** | **0.25 ± 0.03** | **0.18± 0.03** |
| $\tau_3$ (irr. air) | 4.09 ± 0.14 | 4.31 ± 0.16 | 5.09 ± 0.21 | 4.91 ± 0.21 | 4.98± 0.22 |
| **$\tau_3$ (irr. $N_2$)** | **4.22 ± 0.09** | **4.73 ± 0.13** | **4.99 ± 0.20** | **5.04 ± 0.20** | **5.06± 0.09** |

Summary[a] of fluorescence decay parameters of the protein in the irradiated BLG/TPPS complex in air and in $N_2$. $\lambda_{ex}$ = 295 nm, $\lambda_{em}$ = 330 ± 4 nm. Data show a comparison of selected decay parameters. The fluorescence decay was analyzed using three decay components. The complete results can be seen in the supplemental materials.

The investigation of the contribution of the emission band that appears at 405 nm after irradiation could not be investigated because the pulsed light sources available in our laboratory would excite a large contribution of the protein fluorescence even at an emission greater than 400 nm.

**Circular Dichroism in air saturated samples**.

*450-320 NM (TPPS)*. No CD activity can be observed for TPPS bound to BLG, in agreement with the fact that binding to BLG occurs without large distortions of the porphyrin ring.[41,42] Irradiation of TPPS does not induce any CD activity of the porphyrin, indicating that photo-induced mechanisms between TPPS and BLG do not produce new optically active species of the porphyrin or distort its structure.

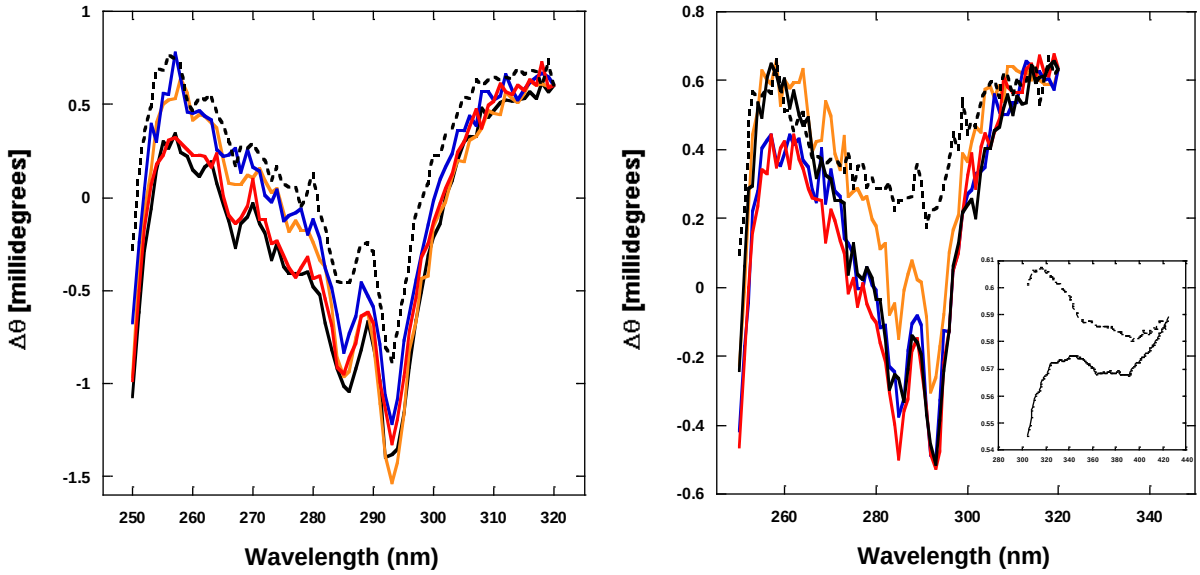


**Figure 18 CD spectrum of the aromatic amino acids region (250-320 nm). Black Solid = BLG/TPPS complex before irradiation; Blue = BLG before irradiation; Orange = BLG after irradiation (3.6 J/cm$^2$); Red = BLG/TPPS complex non-irradiated; Black dashed = BLG/TPPS complex after irradiation (3.6 J/cm$^2$). (Left) pH 6. (Right) pH 9. The insert in (Right) is the overlap of the spectra of the non irradiated complex (solid) and the irradiated complex (dashed) in the 310-420 nm region of the photoproduct and the porphyrin**

*320-250 nm (Aromatic Amino Acids)*. The spectra show negative peaks at 286 and 293 nm due to Trp residues and other negative peaks between 280 and 260 nm due to Tyr residues[43,44] (Figure 18A). At pH ≤ 7 irradiation of the complex prompts a small decrease in the CD negative intensity and a < 10% increase of the ratio between the negative peaks at 293 nm and 286 nm, in comparison with the non-irradiated complex as well as the irradiated and non-irradiated BLG. This indicates some changes in the Trp residues or in their interaction with proximal groups. At alkaline pH, the difference is more dramatic. As Figure 6B shows, the signature double-peak (293 nm, 286 nm) of Trp residues decreases drastically while at the same time a broad peak centered near 321 nm appears (inset of Figure 18B). This is an indication that the Trp residues may have been chemically modified.

*250-196 NM (PROTEIN BACKBONE), Before Irradiation*. The experiments only yielded quality data between 250 and 195 nm. This was due to path length attenuation in the cell. Future work will incorporate a modified short-path cell and improved flow rates.

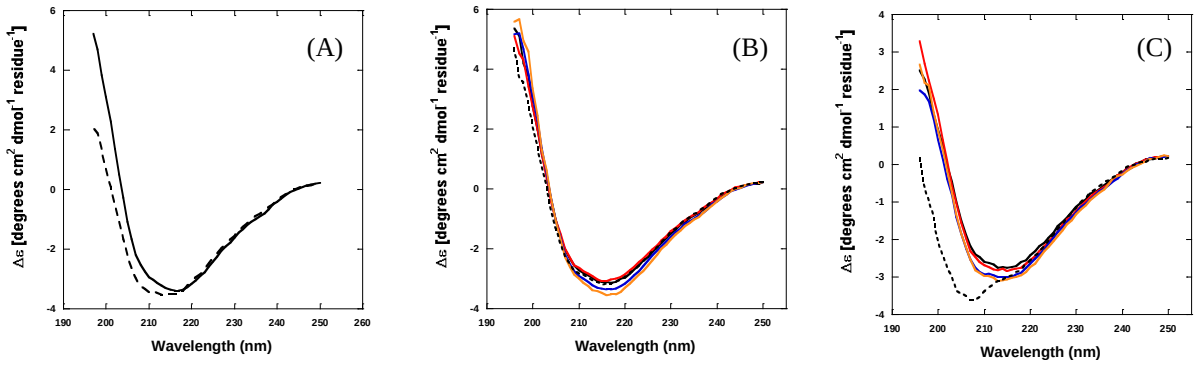


**Figure 19 CD spectra in the region of the secondary structure of the protein (195-250 nm). (A) Spectra of BLG at pH 6 (solid) and pH 9 (dashed). (B) Comparison of spectra at pH 6, air-saturated solutions. Black Solid = BLG/TPPS complex before irradiation; Blue = BLG before irradiation; Orange = BLG after irradiation (3.6 J/cm$^2$); Red = BLG/TPPS complex non-irradiated; Black dashed = BLG/TPPS complex after irradiation (3.6 J/cm$^2$). (C) Comparison of spectra at pH 9, air-saturated solutions. The color scheme is the same as for (B)**

Although this range excludes a portion of the spectrum important for the analysis of the secondary structure [45] our analysis is comparable to the ones reported before for CD spectra at $\lambda > 200$ nm.[46] First of all, it should be noted that the spectra of BLG (alone or in the complex) at alkaline pH are slightly different from the ones at pH 7 and below. The spectrum maintains largely the fingerprint of *β*-conformation (> 55% between sheets and turns (Table 2)) a small shift to lower wavelengths at pH ≥ 8 (Figure 19A) indicates a slight, but above the experimental error, increase (~ 7%) in unordered (random coil) at the expense of β-conformation (Table 7), as calculated with CDPro spectral analysis of the CD signal. This is an indication of a diminished stability of the protein at higher pH as it has been suggested in the past.[27, 47]

*After irradiation*. Figure 19B shows that at pH ≤ 7 there is a nearly perfect overlap between the spectra of the protein and the complex before and after laser irradiation. This indicates that there are no extensive structural effects in BLG. At pH ≥ 8, however, the spectra of the irradiated TPPS/BLG complex show a larger negative peak which shifts from 215 nm to 207 nm. Spectral analysis with CDPro reveals a large increase in the contribution of unordered structure (from 34% to 43%) and an overall decrease of the *β*-sheet + *β*-turn contribution (from 54% to 48%), while the contribution of the helices remains constant (Table 7). This effect is similar, but larger in scale, to the one shown by Qi et al.[45] for the unfolding of BLG at T > 60 ˚C.

*Circular Dichroism in deoxygenated samples.* In comparison with samples in air, eliminating $O_2$ form the solution does not produce any difference in the CD spectra regardless of the pH of the solution or the spectral range. However, our focus was to establish whether $O_2$ is necessary to prompt the large photo-induced CD changes observed in air at alkaline pH. As Figure 20 shows, the irradiation-induced conformational change of BLG in the complex still occurs to nearly the same extent as it does in air-saturated samples (Table 2). This result is in agreement with the fluorescence decay data and show that $O_2$ is not necessary to prompt the conformational rearrangement of the protein.

**Table 7 Results of deconvolution of CD spectra**

| pH 6 (air) | α (%) | β (%) | Turn (%) | Random (%) |
|---|---|---|---|---|
| *BLG non irradiated* | 0.106 ± 0.06 | 0.375 ± 0.08 | 0.205 ± 0.02 | 0.312 ± 0.06 |
| *BLG after irradiation* | 0.123 ± 0.08 | 0.401 ± 0.10 | 0.198 ± 0.06 | 0.287 ± 0.04 |
| *BLG/TPPS before irradiation* | 0.090 ± 0.02 | 0.387 ± 0.04 | 0.199 ± 0.03 | 0.307 ± 0.08 |
| *BLG/TPPS non irradiated* | 0.087 ± 0.03 | 0.375 ± 0.04 | 0.203 ± 0.04 | 0.303 ± 0.09 |
| *BLG/TPPS after irradiation* | 0.092 ± 0.04 | 0.361 ± 0.04 | 0.201 ± 0.05 | 0.308 ± 0.06 |
| **pH 9 (air)** | | | | |
| *BLG non irradiated* | 0.073 ± 0.03 | 0.363 ± 0.06 | 0.196 ± 0.03 | 0.334 ± 0.16 |
| *BLG after irradiation* | 0.113 ± 0.07 | 0.324 ± 0.08 | 0.210 ± 0.02 | 0.350 ± 0.09 |
| *BLG/TPPS before irradiation* | 0.103 ± 0.07 | 0.334 ± 0.08 | 0.208 ± 0.02 | 0.351 ± 0.08 |
| *BLG/TPPS non irradiated* | 0.117 ± 0.08 | 0.338 ± 0.05 | 0.205 ± 0.02 | 0.339 ± 0.09 |
| *BLG/TPPS after irradiation* | 0.100 ± 0.06 | 0.285 ± 0.06 | 0.180 ± 0.02 | 0.432 ± 0.03 |
| **pH 9 (nitrogen)** | | | | |
| *BLG/TPPS before irradiation* | 0.110 ± 0.07 | 0.335 ± 0.08 | 0.210 ± 0.02 | 0.341 ± 0.08 |
| *BLG/TPPS non irradiated* | 0.068 ± 0.03 | 0.339 ± 0.06 | 0.209 ± 0.02 | 0.337 ± 0.06 |
| *BLG/TPPS after irradiation* | 0.079 ± 0.04 | 0.297 ± 0.06 | 0.202 ± 0.03 | 0.419 ± 0.08 |

Analysis of the CD spectra of BLG and TPPS/BLG complexes using CDpro (CDSSTR, CONTNILL, SELCON). Data are presented as percentages of each secondary structure ± S.D.

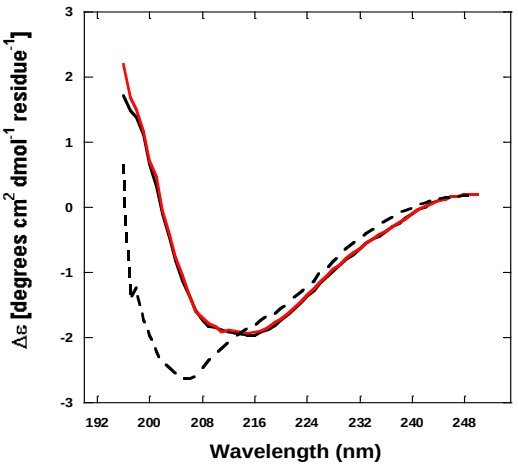


**Figure 20 Comparison of spectra at pH 9, $N_2$-saturated solutions. Black Solid = BLG/TPPS complex before irradiation; Red = BLG/TPPS complex non-irradiated; Black dashed = BLG/TPPS complex after irradiation (3.6 J/cm$^2$)**

*Capillary liquid chromatography-mass spectrometry (LC/MS) and –tandem mass spectrometry (LC/MS/MS).* The intact average mass of BLG, as determined by capillary LC/MS and maximum entropy deconvolution of the electrospray charge state envelope, was 18,278 Da (Figure 21). This is in excellent agreement, with less than a 1 Da or 55 ppm mass error, with the theoretical average mass of the amino acid sequence for gi|6729725 (NCBI sequence database) at 18,277 Da (Figure 21-inset).

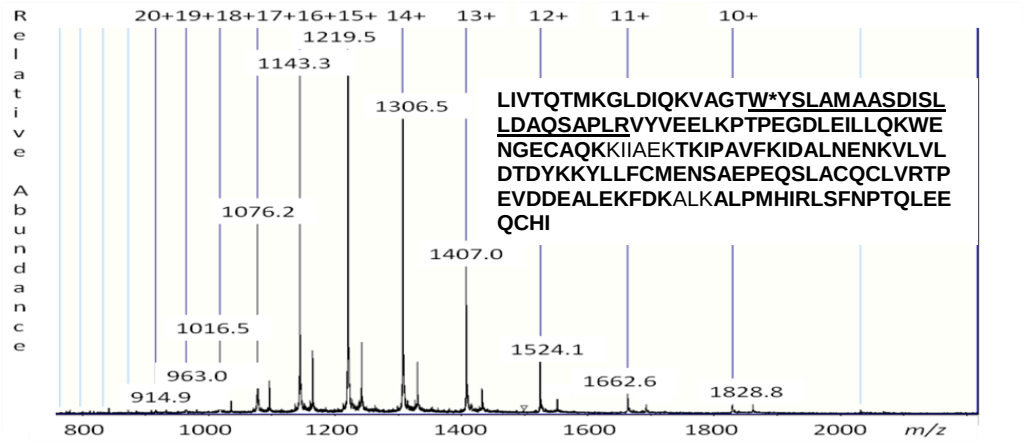


**Figure 21 The intact average mass of BLG, as determined by capillary LC/MS and maximum entropy deconvolution of the electrospray charge state envelope, was 18,278 Da. This is in excellent agreement with the theoretical average mass of the amino acid sequence for gi|6729725 at 18,277 Da (inset)**

The charge state envelope for BLG spanned from $[m+20H]^{20+}$ to $[m+10H]^{10+}$ with the most abundant charge state ($[m+15H]^{15+}$) at *m/z* 1219.5. The minor, unlabeled, peaks in Figure 8A correspond to an unknown protein impurity present at less than 10% the relative abundance of BLG in both non-irradiated and irradiated samples. The amino acid sequence of BLG, as determined by capillary LC/MS/MS of tryptic digests and probability-based protein database searching of MS/MS spectra,[48] was identified as gi|6729725 with 94% sequence coverage (Figure 21-inset). Tryptic peptides with an MS/MS spectrum that could be assigned to BLG are shown in bold. Significantly, tryptic peptides spanning both Trp19 (underlined) and 61 were observed. Error tolerant protein database searching[49] of MS/MS spectra from capillary LC/MS/MS of tryptic digests of irradiated BLG samples showed a +19.99 Da modification of Trp19 to hydroxykynurenine (OHKyn) in a tryptic peptide spanning amino acid residues 15-40 (Figure 22).

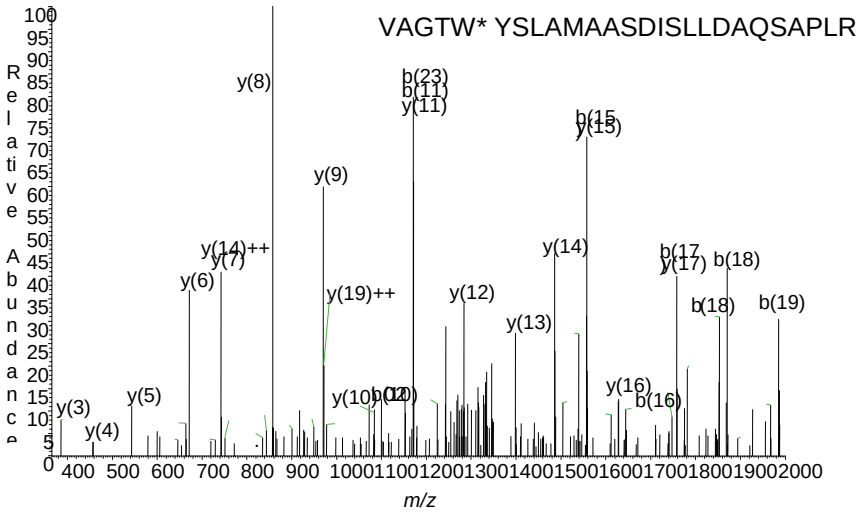


**Figure 22 Error tolerant protein database searching of MS/MS spectra from capillary LC/MS/MS of tryptic digests of irradiated BLG samples showed a +19.99 Da modification of Tryptophan 19 to hydroxykynurenine (OHKyn) in a tryptic peptide spanning amino acid residues 15-40. The observed monoisotopic mass of this OHKyn-modified tryptic peptide, with amino acid sequence VAGTW*YSLAMAASDISLLDAQSAPLR, was 2726.70 Da. This is in excellent agreement with the theoretical monoisotopic mass. Likewise, the OHKyn assignment to Trp 19 is in excellent agreement with the theoretical monoisotopic masses for gas-phase fragmentation of this OHKyn-modified tryptic peptide**

The theoretical monoisotopic mass of the unmodified- and OHKyn -modified forms of this tryptic peptide is 2706.37 Da and 2726.36 Da, respectively. The observed monoisotopic mass of the OHKyn-modified tryptic peptide, with amino acid sequence VAGTW*YSLAMAASDISLLDAQSAPLR, was 2726.70 Da. This is in excellent agreement, with less than a 127 ppm (precursor ion) mass error, with the theoretical monoisotopic mass. Likewise, the OHKyn assignment to Trp 19 is in excellent agreement, with less than a 272 ppm (product ion rms) mass error, with the theoretical monoisotopic masses for gas-phase fragmentation (CID) of this OHKyn-modified tryptic peptide. Lastly, confidence in our MS/MS assignments is reflected by the low expectation values of 1.3E-7 for this OHKyn-modified tryptic peptide, observation of 15 OHKyn-specific product ions, and observation of the oxidized-methionine form of this peptide (data not shown) , respectively.

# 4 Conclusions

The data recorded with our measurements established several important "landmarks" for the study of the interaction of porphyrins with globular proteins. Porphyrins appear to prefer binding to superficial location on both BLG and tubulin. In the case of BLG and PPIX, this location is modulated by the pH-induced conformational change of the protein, while in the case of the negatively-charged TPPS, binding is not affected by the conformational change of BLG.

In summary, our results show that both porphyrins bind tubulin dimers with the same stoichiometry but with higher affinity for the water soluble TSPP through the formation of at least one ionic interaction. Our results also indicate that binding sites may be separate for the two porphyrins and do not seem to overlap with the sites of other known tubulin ligands. Direct evidence for this is however not available yet since initial attempts of studying binding competition between PPIX and TSPP using optical methods was unsuccessful due to the overlap of the absorption and emission spectra of the two porphyrins. Thus, additional investigations are ongoing to establish the exact location of the binding sites and the effect of porphyrins on tubulin *in vitro* polymerization. This first study shows that understanding the interaction between tubulin and porphyrins may in the future offer a mechanistic explanation of the porphyrin-induced damage of microtubules and for the advancement of the use of porphyrins in phototherapy.

Our results show that porphyrins such as PPIX are indeed capable of modifying the structure of non-specific proteins upon irradiation of the Soret band. Although more detailed mechanistic studies are necessary, these results suggest that (a) phototoxicity of porphyrins may proceed through direct reaction with target proteins and (b) porphyrins may be used to trigger conformational changes useful for the investigation of protein folding/unfolding mechanisms. The unfolding mechanism is not $O_2$-dependent, therefore a direct charge transfer between the porphyrin and one amino acid in the binding site is the likely cause of the conformational change rather than a more "trivial" oxidation produced by PPIX-sensitized singlet oxygen. The fact that the mechanism of photoinduced conformational change does not depend on $O_2$, is extremely important for future development of porphyrin-induced conformational changes of proteins in biomedical applications and in proteomics.

In conclusion we have demonstrated that TPPS, non-covalently attached to a small globular protein (BLG), is capable of mediating photo-induced unfolding of the polypeptide. The unfolding is large (~ 20%) and proceeds through PET between the porphyrin and the protein. This mechanism does not require the mediation of $O_2$ to produce molecular "damage" to the protein and can be categorized as a Type III photosensitization mechanism. Additional investigations are ongoing. However, these results suggest that this property of TPPS can be translated to other porphyrin/protein systems and could be used to prompt photo-induced protein unfolding and protein inactivation as a viable strategy for biomedical applications of porphyrins.

# 5 Acknowledgments

**THE FOLLOWING PEER-REVIEWED PUBLICATIONS WERE PRODUCED AS A RESULT OF THIS GRANT:**

- Fernandez, N.F., Sansone, S., Mazzini, A., **Brancaleon, L.**, **2008**, Irradiation of the porphyrin causes unfolding of the protein in the Protoporphyrin IX/β-lactoglobulin non covalent complex. *The Journal of Physical Chemistry B*. 112:7592-7600. Impact Factor 4.12.

- Silva, I., Sansone, S., **Brancaleon, L.**, **2008**, Monomeric meso-tetraskis(sulphonatophenyl)-porphine binds β-Lactoglobulin A at a superficial site rich in lysine residues, *The Protein Journal*. 28:1-13. Impact Factor 1.01.

- Fernandez, N.F., Sansone, S., Belcher, J., Haskins, W.E., **Brancaleon, L.**, **2008**, Photo-induced unfolding of β-lactoglobulin mediated by a water soluble porphyrin. Submitted to the *The Journal of Physical Chemistry B*. Impact Factor 4.01.

Two additional manuscripts are in preparation and will be submitted for publication before September 2009.

**THE FOLLOWING CONFERENCE PRESENTATIONS WERE PRODUCED AS A RESULT OF THIS GRANT:**

a) ¥Silva, I.*, Sansone, S.M.*, **Brancaleon, L.**, **2007**, 'Fluorescence spectroscopy investigation and molecular docking simulation of the interaction of β-lactoglobulin A (BLGA) with meso-tetrakis(4-sulfonatophenyl) porphyrin (TSPP)' *21st Annual Meeting of the Protein Society*, Boston, MA, USA, July 21-25*.

b) ¥Johnson, E.M.*, Tian, F., **Brancaleon, L.**, **2007**, 'Porphyrins vs. Anti-Microtubule Agents: Photophysical Study of the Interactions and Influence on Tubulin Polymerization', *Annual Biomedical Research Conference for Minority Students (ABRCMS)*, November 8-11, Austin, TX, USA.

c) ¥Johnson, E.M.*, Brancaleon, L., **2008**, 'Effecs of porphyrins on tubulin polymerization', *Annual Meeting of the Biophysical Society*, February 5-12, Long Beach, CA, USA.

d) Brancaleon, L., **2008**, Direct Protein Photoinduced Conformational Changes Using Porphyrins, *March Meeting of the American Physical Society*, March 9-14, New Orleans, LA, USA.

e) Valdez, R.*, Johnson, E.M.*, Tian, F., Brancaleon, L., **2008**, Effects of Porphyrins on Tubulin Polymerization, *34th Meeting of the American Society for Photobiology*, June 20-25, Burlingame, CA, USA.

f) Fuini, J.*, Pennick, M.*, Negrete, G., Brancaleon, L., **2008**, Characterizing the photophysics of new perylene derivatives, *Annual Conference of the Society for Advancement of Chicanos and Native Americans in Science (SACNAS)*, October 9-12, Salt Lake City, UT, USA.

g) ¥Belcher, J.*, Fuini, J.*, Brancaleon, L., **2008**, Tubulin Binding Competition Between Porphyrins and Well-Characterized Ligands**,** *Annual Conference of the Society for Advancement of Chicanos and Native Americans in Science (SACNAS)*, October 9-12, Salt Lake City, UT, USA.

¥ award winning
* students

# 6 References


1. Kessel, D. *Photochem. Photobiol. Sci.* **2002**, *1*, 837.

2. Berg, C., Moan, J. *Photochem. Photobiol.* **1997**, *65*, 403.

3. Scuteri, A., Nicolini, G., Miloso, M., Bossi, M., Cavaletti, G., Windebank, A.J., Tredici, G. *Anticancer Res.* **2006**, *26*, 1065.

4. Loweneck, M., Milbradt, A.G., Root, C., Satzger, H., Zinth, W., Moroder, L., Renner, C. *Biophys. J.* **2006**, *90*, 2099.

5. Eaton, W. A., Munoz, V., Hagen, S.J., Jas, G.S., Lapidus, L.J., Henry, E.R., Hofrichter, J. *Annu. Rev. Biophys. Biomol. Struct.* **2000**, *29*, 327.

6. Nogales, E., Wolf, S.G., Downing, K.H. *Nature* **1998**, *391*, 199.

7. Avila, J. *FASEB J.* **1990**, *4*, 3284.

8. Madiraju, C., Edler, M.C., Hamel, E., Raccor, B.S., Balachandran, R., Zhu, G., Giuliano, K.A., Vogt, A., Shin, Y., Fournier, J.H., Fukui, Y., Bruckner, A.M., Curran, D.P., Day, B.W. *Biochemistry* **2005**, *44*, 15053.

9. Boekelheide, K., Eveleth, J., Tatum, A.H., Winkelman, J.W. *Photochem. Photobiol.* **1987**, *46*, 657.

10. Davies, K. J. A., Lin, S.W., Pacifici, R.E. *J. Biol. Chem.* **1987**, *262*, 9914.

11. Andrade, S. M., Costa, S.M.B. *Biophys. J.* **2002**, *82*, 1607.

12. Maiti, N. C., Ravikanth, M., Mazumdar, S., Periasamy, N. *J. Phys. Chem.* **1995**, *99*, 17192.

13. Horowitz, P., Prasad, V., Luduena, R.F. *J. Biol. Chem.* **1984**, *259*, 14647.

14. Collini, M., D'Alfonso, L., Baldini, G. *Prot. Sci.* **2000**, *9*, 1968.

15. Tulp, A., Verwoerd, D., Hard, A.A. *Electrophoresis* **1997**, *18*, 767.

16. Harvey, B. J., Bell, E., Brancaleon, L. *J. Phys. Chem. B* **2007**, *111*, 2610.

17. Cho, Y., Batt, C.A., Sawyer, L. *J. Biol. Chem.* **1994**, *269*, 11102.

18. Lehrer, S. S. *Biochemistry* **1971**, *10*, 3254.

19. Tian, F., Johnson, K, Lesar, A.E., Moseley, H., Ferguson, J., Samuel, I.D.W., Mazzini, A., Brancaleon, L. *Biochim. Biophys. Acta* **2005**, *1760*, 38.

20. Tian, F., Johnson, E.M, Zamarripa, M., Sansone, S., Brancaleon, L. *Biomacromol.* **2007**, *8*, 3767.

21. Galani, D., Apenten, R.K.O. *Food Res. Internat.* **1999**, *32*, 93.

22. Hamada, D., Dobson, C.M. *Protein Sci.* **2002**, *11*, 2417.

23. Gottschalk, M., Nilsson, H., Roos, H., Halle, B. *Protein Sci.* **2003**, *12*, 2404.

24. Capron, I., Nicolai, T., Durand, D. *Food Hydrocoll.* **1999**, *13*, 1.

25. Folgolari, F., Ragona, L., Zetta, L., Romagnoli, S., De Kruif, K.G., Molinari, H. *FEBS Lett.* **1998**, *436*, 149.

26. Brownlow, S., Morais Cabral, J.H., Cooper, R., Flower, D.R., Yewdall, S.J., Polikarpov, I., North, A.C.T., Sawyer, L. *Structure* **1997**, *5*, 481.

27. Qin, B. Y., Bewley, M.C., Creamer, L.K., Baker, H.M., Baker, E.N., Jameson, G.B. *Biochemistry* **1998**, *37*, 14014.

28. Fessas, D., Iametti, S., Schiraldi, A., Bonomi, F. *Eur. J. Biochem.* **2001**, *268*, 5439.

29. Beltramini, M., Firey, P.A., Ricchelli, F., Rodgers, M.A.J., Jori, G. *Biochemistry* **1987**, *26*, 6852.

30. Ricchelli, F., Stevanin, D., Jori, G. *Photochem. Photobiol.* **1988**, *48*, 13.

31. Brancaleon, L., Magennis, S.W., Samuel, I.D.W., Namdas, E., Lesar, A., Moseley, H. *Biophys. Chem.* **2004**, *109*, 351.

32. Dahms, T. E. S., Willis, K.J., Szabo, A.G. *J. Am. Chem. Soc.* **1995**, *117*, 2321.

33. Samanta, U., Pal, D., Chakrabarti, P. *Proteins* **2000**, *38*, 288.

34. Tanaka, F., Kaneda, N., Mataga, N., Tamai, N., Yamazaki, I., Hayashi, K. *J. Phys. Chem.* **1987**, *91*, 6344.

35. Ross, J. B. A., Schmidt, C.J., Brand, L. *Biochemistry* **1981**, *20*, 4369.

36. Brancaleon, L., Moseley, H. *Biophys. Chem.* **2002**, *96*, 77.

37. Ricchelli, F., Gobbo, S., Moreno, G., Salet, C., Brancaleon, L., Mazzini, A. *Eur.J. Biochem.* **1998**, *253*, 760.

38. Hall, D., Minton, A.P. *Anal. Biochem.* **2005**, *345*, 198.

39. Stryer, L. *Ann. Rev. Biochem.* **1978**, *47*, 819.

40. Eftink, M. R., C.A. Ghiron. *Anal. Biochem.* **1981**, *114*, 189.

41. Pasternack, R. F. *Chirality* **2003**, *15*, 329–332.

42. Kurtan, T., Nesnas, N., Koehn, F.E., Li, Y.Q., Nakanishi, K., Berova, N. *J. Am. Chem. Soc.* **2001**, *123*, 5974.

43. Rasmussen, P., Barbiroli, A., Bonomi, F., Faoro, F., Ferranti, P., Iriti, M., Picariello, G., Iametti, S. *Biopolymers* **2007**, *86*, 57.

44. Zhang, X., Keiderling, T.A. *Biochemistry* **2006**, *45*, 8444.

45. Qi, X. L., Holt, C., McNulty, D., Clarke, D.T., Brownlow, S., Jones, G.R. *Biochem. J.* **1997**, *324*, 341.

46. Crougennec, T., Molle, D., Mehra, R., Bouhallab, S. *Protein Sci.* **2004**, *13*, 1340.

47. Taulier, N., Chalikian, T.V. *J. Mol. Biol.* **2001**, *314*, 873.

48. Perkins, D. N., Pappin, D.J., Creasy, D.M., Cottrell, J.S. *Electrophoresis* **1999**, *20*, 3551.

49. Creasy, D. M., Cottrell, J.S. *Proteomics* **2002**, *2*, 1426.